Ocean Dynamics (2012) 62:1153–1167
DOI 10.1007/s10236-012-0552-6

Tides, sea-level rise and tidal power extraction on the European shelf

Sophie L. Ward · J. A. Mattias Green · Holly E. Pelling

Received: 6 February 2012 / Accepted: 14 May 2012 / Published online: 27 June 2012

Abstract An established numerical tidal model has been used to investigate the impact of various sea-level rise (SLR) scenarios, as well as SLR in combination with large-scale tidal power plants on European shelf tidal dynamics. Even moderate and realistic levels of future SLR are shown to have significant impacts on the tidal dynamics of the area. These changes are further enhanced when SLR and tidal power plants are considered in combination, resulting in changes to tidal amplitudes, currents and associated tidal dissipation and bed shear stresses. Sea-level rise is the dominant influence on any far-field impacts, whereas tidal power plants are shown to have the prevailing influence over any changes close to the point of energy extraction. The spatial extent of the impacts of energy extraction is shown to be affected by the sea level when more than one tidal power plant in the Irish Sea was considered. Different ways to implement SLR in the model are also discussed and shown to be of great significance for the response of the tides.

Keywords Tides · Sea-level rise · Tidal power · Tidal model · European shelf

Responsible Editor: Joachim W. Dippner

S. L. Ward (✉) · J. A. M. Green · H. E. Pelling
School of Ocean Sciences, College of Natural Sciences, Bangor University, Menai Bridge, LL59 5AB, UK
e-mail: ospa1a@bangor.ac.uk

1 Introduction

The environmental, economic and socioeconomic impacts of sea-level rise (SLR) make it one of the most serious issues associated with climate change. With around 200 million people living in coastal floodplains worldwide (Milne et al. 2009), atmospheric warming of 3 to 4 °C could result in the flooding of the homes of tens to hundreds of thousands more people each year (Stern 2007). There is significant evidence to suggest that global mean sea level is currently rising significantly, after a period of little or no increase for almost 2,000 years (e.g. Gehrels et al. 2004; Miller and Douglas 2004; Church and White 2006; Bindoff et al. 2007). Here, we investigate how sea levels of up to 5 m above present-day levels, in combination with tidal energy extraction by large-scale tidal power plants, influence the tide on the northwest European shelf.

Bindoff et al. (2007) predicted a SLR of between 0.75 and 1.9 m for the period 1990–2100. By linking sea levels to global temperatures, Vermeer and Rahmstorf (2009) concluded that by 2100, sea levels could actually rise by approximately three times that estimated by Bindoff et al. (2007); however, due to geological constraints, sea level is very unlikely to increase by more than 2 m by 2100 (Pfeffer et al. 2008). There is still significant variability in future sea level predictions, attributable to uncertainties in ice flow dynamics, contribution of terrestrial water sources and anthropogenic water storage (Bindoff et al. 2007; Hunter 2009; Milne et al. 2009; Gehrels 2010). Contributions of land ice also contain inherent uncertainty due to the lack of information regarding total ice volume and likely melt rates, as well as uncertainties in predicting likely changes in global atmospheric temperatures for the twenty-first

century (Nerem et al. 2006; Vermeer and Rahmstorf 2009).

The areal extent of the shelf seas, which have average depths of less than 200 m, is currently around 7% of the total global sea surface. Significant changes in sea levels have influenced the tidal regimes in the past (Egbert et al. 2004; Uehara et al. 2006; Green 2010), with consequences for the location of tidal mixing fronts and levels of tidally driven mixing (Uehara et al. 2006), changes in wave climates (Neill et al. 2009a) and indirectly shelf sea biogeochemistry (Rippeth et al. 2008) and sediment transport (van der Molen 2002; Hall and Davies 2004; Lane and Prandle 2007; Van Landeghem et al. 2009).

A number of modelling studies have been conducted into how past changes in SLR have altered the global tides (e.g. Egbert et al. 2004; Uehara et al. 2006; Griffiths and Peltier 2008; Green et al. 2009; Griffiths and Peltier 2009; Muller et al. 2010). There have not, however, been any regional studies of the effect of SLR on the tides on the European shelf with the exception of Pickering et al. (2012), who presents some surprising results. They show that even moderate SLR (up to 1 m) may have significant impact on the tides on the European shelf, changing the tidal amplitudes with tens of centimetres from present-day levels. Furthermore, the responses vary greatly between different locations in both magnitude and sign of the change.

There has been rapidly growing interest in tidal energy in recent years. The two distinct categories of tidal resource are tidal range (e.g. barrages and lagoons) and tidal stream (e.g. free stream turbines). In recent years, a variety of studies have been carried out into impacts of tidal energy extraction by using zero-dimensional and two-dimensional numerical models (e.g. Sutherland et al. 2007; Burrows et al. 2009a; Neill et al. 2009b; Prandle 2009; Wolf et al. 2009; Xia et al. 2010) and more lately using a three-dimensional model (Hasegawa et al. 2011). Tidal power plants (TPPs) can be crudely represented within tidal models by increasing the bed friction by modifying the drag coefficient (e.g. Sutherland et al. 2007; Arbic and Garrett 2009), thus increasing the amount of energy dissipation that occurs in the location of the TPP. Restricting the flow of the water using turbines can have feedback effects on the tides, by affecting both the mean water level within a basin and by causing a decrease in tidal current speeds, with dual mode having less severe impacts than the single flood or ebb generation modes (Sutherland et al. 2007; Burrows et al. 2009a; Neill et al. 2009b). The number of turbines and the corresponding power output must thus be carefully considered when identifying potentially suitable areas and planning the installation of TPPs (e.g. Sutherland et al. 2007; Prandle 2009; Ross 2011). Neill et al. (2009b) found that the effect on the tides of free stream turbines in the Severn Estuary did not extend beyond the head of the estuary, i.e. no further than 50 km from the location of energy extraction. A similar response was found by Wolf et al. (2009) with a barrage in the Severn Estuary. The results of the study by Wolf et al. (2009) suggested that with barrages in five estuaries in the Irish Sea, there was an increase in tidal amplitude along the east coast of Ireland, which could have implications for coastal flooding.

In this paper, we present the results from a numerical modelling study on the impacts of future SLR, in combination with TPP, on the tides on the European shelf, which are located on the northeastern margin of the North Atlantic (Fig. 1). The tides in the area are predominantly semi-diurnal (Pingree and Griffiths 1982) and a co-oscillating response of the shelf seas to the tides generated in the Atlantic Ocean. Tidal energy from the Atlantic is transmitted onto the European shelf into the Celtic Sea between Brittany and southern Ireland via the Atlantic semidiurnal Kelvin wave, which travels south to north. The wave propagates into the English Channel and some is passed into the southern North Sea, the Irish Sea and into the Bristol Channel (Pugh 1996). The north of Scotland diffracts part of the semidiurnal wave, and it turns east and to the south into the North Sea. The diurnal tide behaves as a standing wave in the Celtic Sea, the Bristol Channel and English Channel, but without any tendency to resonance (Pugh 1996). The semi-diurnal constituents, M_2 and S_2, domi-

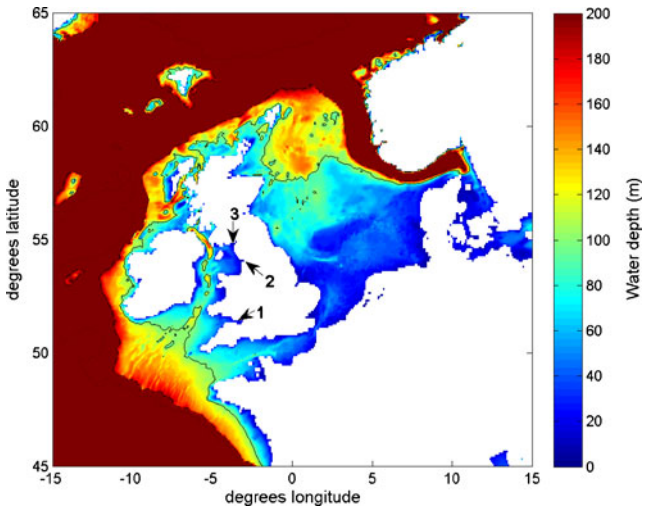

Fig. 1 The northwest European continental shelf and shelf seas with depth contours plotted at water depths of 100 m (*solid line*), 200 m (*dashed line*) and 1,000 m (*dotted line*). *Arrows* to the UK estuaries/bays discussed in the paper mark (1) Severn Estuary, (2) Morecambe Bay and (3) Solway Firth

nate the tidal regime on the northwest European shelf, although consideration of M_2 and M_4 is most significant for sediment transport on the shelf (e.g. Pingree and Griffiths 1979). Only near semi-diurnal amphidromes and in limited regions are diurnal constituents such as K_1 and O_1 comparable with the semi-diurnal constituents (Pugh 1996). The northwest European shelf dissipates some 200 GW of tidal energy, or 5 to 6% of the total present-day global tidal dissipation, making it the second most energetic shelf on the planet (Egbert and Ray 2001).

In this study, a series of model simulations were conducted for a range of possible SLR scenarios, including an extreme of 5 m. Increased sea levels above present day were considered in parallel with large-scale TPPs in order to consider the combined impact of increased water depths and energy extraction on the tidal dynamics on the shelf. The model is presented in the following section. Section 3 outlines how SLR was implemented within the model and the results of the SLR runs, which are presented as impact on tides and hence on energy dissipation and bed shear stresses. Section 4 outlines the parameterisation and implementation of large-scale tidal power plants within the model and the effect on the tides when energy extraction is considered in combination with SLR. The discussion and conclusions are presented in Section 5.

2 Model description

2.1 Shelf model

Shelf-scale numerical modelling was undertaken using Kyushu University's Tidal Model (KUTM) (Uehara et al. 2006), a two-dimensional finite-difference model which was run with a resolution of 1/12° over the northwest European shelf, encompassing latitudes from 45° N to 65° N and longitudes from 15° W to 15° E (Fig. 1). The KUTM model is well-established and has been shown to provide good results for the area of interest (Uehara et al. 2006), with a lower RMS error than many other models when compared to observations. Assuming shallow water dynamics, the governing equations are given by:

$$\frac{\partial \eta}{\partial t} + \nabla \cdot (D\mathbf{u}) = 0 \tag{1}$$

$$\frac{\partial D\mathbf{u}}{\partial t} + (\mathbf{u} \cdot \nabla) D\mathbf{u} + \mathbf{k} f \times D\mathbf{u} = -gD\nabla(\eta - \eta_e) - c_d|\mathbf{u}|\mathbf{u} + A_h D\nabla^2\mathbf{u} \tag{2}$$

where $\mathbf{u}$ is the velocity vector, t is time, ∇ the horizontal gradient operator, η is the surface elevation, $D = H + \eta$ where H is the undisturbed depth, f is the Coriolis parameter, $\mathbf{k}$ the vertical unit vector, g the acceleration due to gravity, η_e the tide-generating potential, c_d the bed friction coefficient and A_h the horizontal eddy-viscosity coefficient ($= 100$ m^2 s^{-1}). The bottom friction coefficient was set to 2×10^{-3}, although runs with a reasonable range of values did not provide any significant difference. The model allows the flooding of land cells with increasing sea levels.

The bathymetry for the modern-day northwest European shelf had previously been prepared by Uehara et al. (2006) by compiling data from sources including the UK Proudman Oceanographic Laboratory, the British Geological Survey and the US National Geophysical Data Center. The model is forced by surface elevation and depth-mean currents along the open boundaries (taken from TPXO.6, Egbert and Erofeeva 2002) and by the astronomical tidal potential for the M_2, S_2, N_2, K_1 and O_1 constituents over the domain. Further details can be found in Uehara et al. (2006). Each run was initiated from rest and integrated for 45 days. The first 15 of these were omitted from the subsequent harmonic analysis.

The model outputs the amplitude, phase and depth-mean tidal velocities of the forcing constituents and the quarter-diurnal constituent, M_4 (note that M_4 is not included in the forcing). The tidal velocities were used to calculate bed shear stress (τ) and tidal dissipation (ϵ) from

$$\tau = \rho c_d |u|^2 \tag{3}$$

and

$$\epsilon = \rho c_d |u|^3 \tag{4}$$

Both the average and peak tidal velocities in the flood (positive) and ebb (negative) directions were outputted by the model and used to calculate the bed shear stress, and the absolute tidal velocities were used to calculate the dissipation.

2.2 Simulations

Control runs (shown in Figs. 2, 3, 4, 5 and 6 and discussed in context below) were conducted using present-day sea levels, and these model outputs were validated by comparison with the results of previous investigations of the region (e.g. Pingree and Griffiths 1979; Hall and Davies 2004; Uehara et al. 2006; Mitchell et al. 2010). The root mean squared (RMS) error of the model is less than 6 cm and 6.5° for the M_2 amplitude

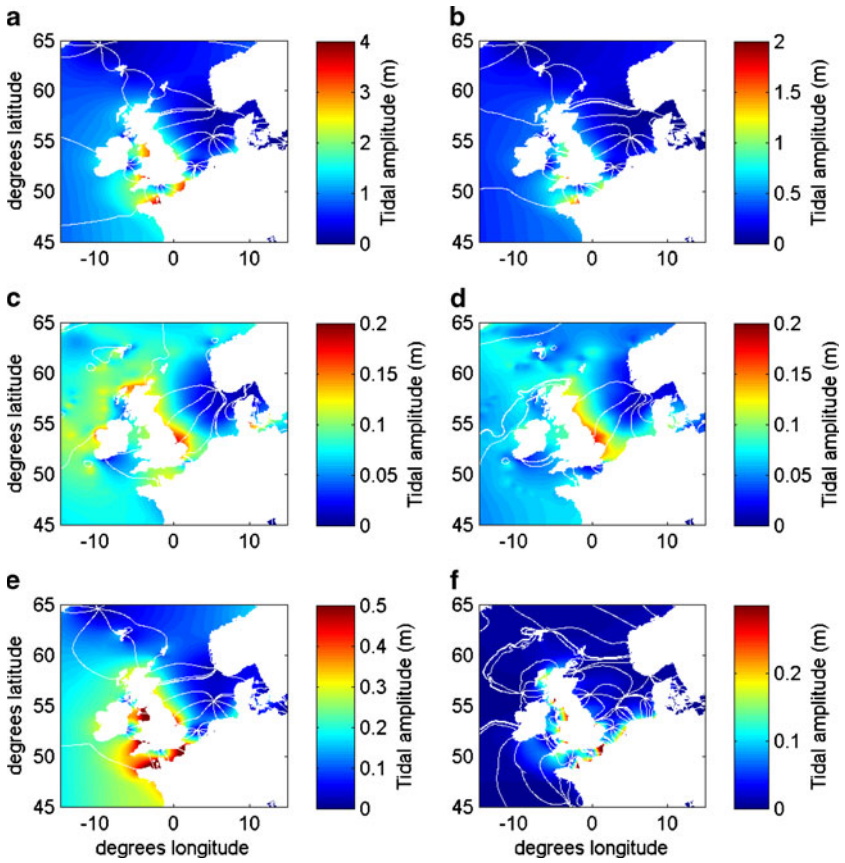

Fig. 2 Amplitudes and phases for all constituents considered within the model, shown for present-day sea level (control run), where **a** M_2, **b** S_2, **c** K_1, **d** O_1, **e** N_2 and **f** M_4. Note the different scales

and phase, respectively (see Uehara et al. 2006, for details), and 4 cm for the M_4 amplitude. Model validation is discussed further in Pelling et al. (2012), where it is shown that the tidal amplitudes of the control runs compare well with the OTIS-ATLAS (available at http://volkov.oce.orst.edu/tides/ES.html). Any modelled changes less than the RMS errors were considered negligible and are not included for discussion in the results section.

The results of the SLR simulations focus on the changing tidal amplitudes of the M_2 and M_4 tidal constituents. Since the tides on the European shelf are completely dominated by the semi-diurnal tides and its harmonics, we chose to focus on effects on M_2 and M_4 in the following. Note that the M_4 amplitude exceeds 50 cm at several locations in the area (Andersen 1999, and our Fig. 2).

3 Impact of sea-level rise on the tides

3.1 Methods

Varying the sea level within the model altered the level uniformly across the entire domain and allowed the formation of new sea cells as a result of flooding of land cells. Where the SLR was not great enough to flood an entire cell, a solid vertical wall was assumed at the present land-sea boundary. Note that the bathymetric database also contains topography and hence the elevation of the land cells is considered. With 2-m SLR, the flooding of land cells was observed in a number of estuaries around the British coast as well as along the northern coast of Holland and in the German Bight. With 5-m SLR, in addition to these areas, there was also significant generation of new sea cells in the areas of the Severn Estuary (UK), in the Kattegat and along the northwestern coast of France.

The focus was on the comparison of 2- and 5-m SLR and present-day conditions (where 5 m is considered an extreme worst-case scenario (Vermeer and Rahmstorf 2009)) although a number of different increased and decreased sea level scenarios were investigated, i.e. 1 and 2 m below present-day level and 1, 3 and 4 m above present-day level. Presented in this section are the comparisons between the present-day (the control run) and the 2- and 5-m SLR scenarios. The SLR figures have been generated in such a way that it is the difference between the SLR scenario and present-day conditions

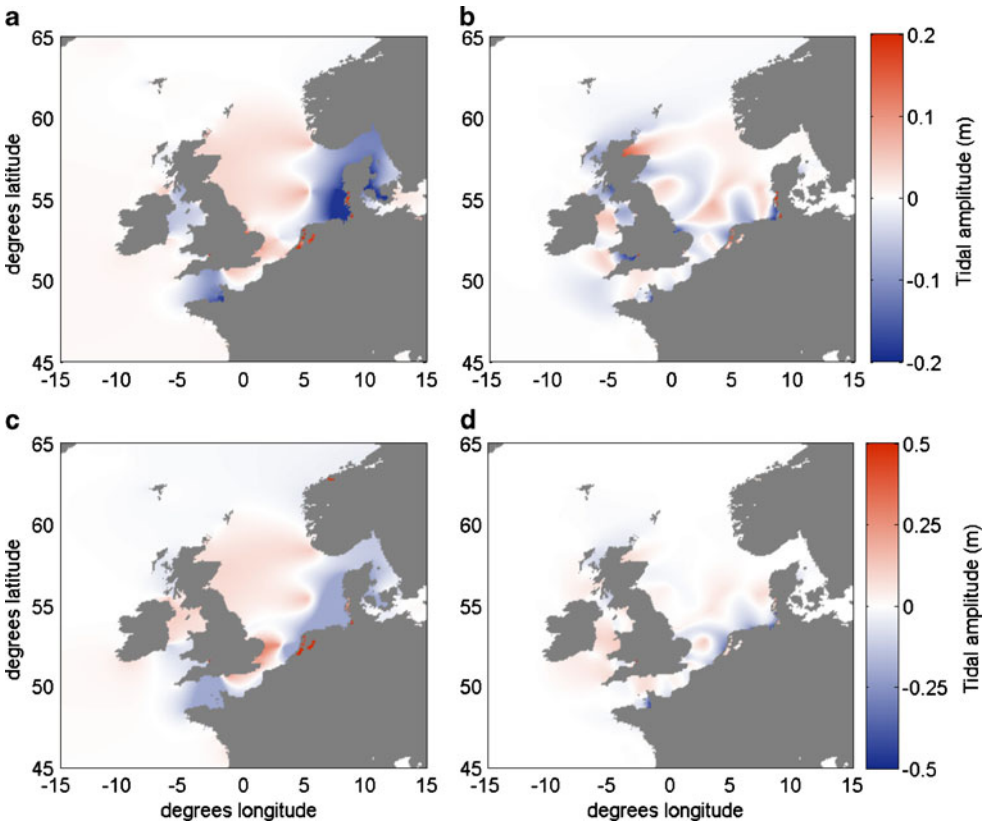

Fig. 3 Difference between M_2 (**a**, **c**) and M_4 (**b**, **d**) amplitudes for the 2 m (**a**, **b**) and 5 m (**c**, **d**) SLR scenarios and present day. Note the different scales for the *upper* and *lower panels*. In both M_4 plots, the difference has been multiplied by factor 2 for better visualisation

that is presented. Present day phases and amplitudes are presented in Fig. 2.

3.2 Results: tidal amplitudes and phases

The response of the tides to increasing sea levels displayed considerable spatial variability (Fig. 3). The very red grid cells along the Dutch coast indicate where former land cells are flooded with SLR. SLR response curves (Figs. 4 and 5) have been plotted for a number of points within the domain and show actual and percent of present-day change of M_2 and M_4 amplitudes. Between present day and 2-m SLR, there was a significant decrease in M_2 amplitudes in the Irish Sea (3%), in the area of the Channel Isles (6%) and in Pentland Firth, Scotland (7%), the latter being an area being considered for a free stream tidal energy plant. The variation in the tidal amplitudes in the western Irish Sea between present day and SLR scenarios suggests that the resonance in the Irish Sea will occur at extreme SLR (e.g. 5 m). Only the point taken in the English Channel displayed an increase in M_2 amplitude (of 2%) between 2-m SLR and the control. The area of most significant decrease in M_2 tidal amplitudes was the German Bight with a SLR of 5 m; here the amplitude decreased by almost 50% from present-day value of approximately 1.7 m. The increase in tidal amplitude observed in the open water on the shelf is influenced by the weaker currents resulting from higher water levels, which lead to weaker damping.

In order to quantify the effects of SLR on the tides, we consider the migration of amphidromic points. The M_2 amphidromic point, which lies in the eastern North Sea at present, moved increasingly eastwards with rising sea levels, approximately 32 and 90 km with 2- and 5-m SLR, respectively. With 5-m SLR, there was also an eastwards shift of almost 40 km of the M_2 amphidrome situated to the northeast of the English Channel. The shift of this amphidromic point is likely to be a significant factor in the response of the tidal amplitudes along the eastern coast of the UK.

Two present-day M_4 amphidromic points in the southern North Sea were not present in the 2- nor the 5-m SLR model results. There was a northwesterly shift of approximately 22 km of the M_4 amphidrome situated between the southern Irish Sea and just off the coast of Cornwall (England), with 5-m SLR. The present-day M_4 amphidrome in the Moray Firth (Scotland) did not exist in the 5-m SLR scenario, although a new

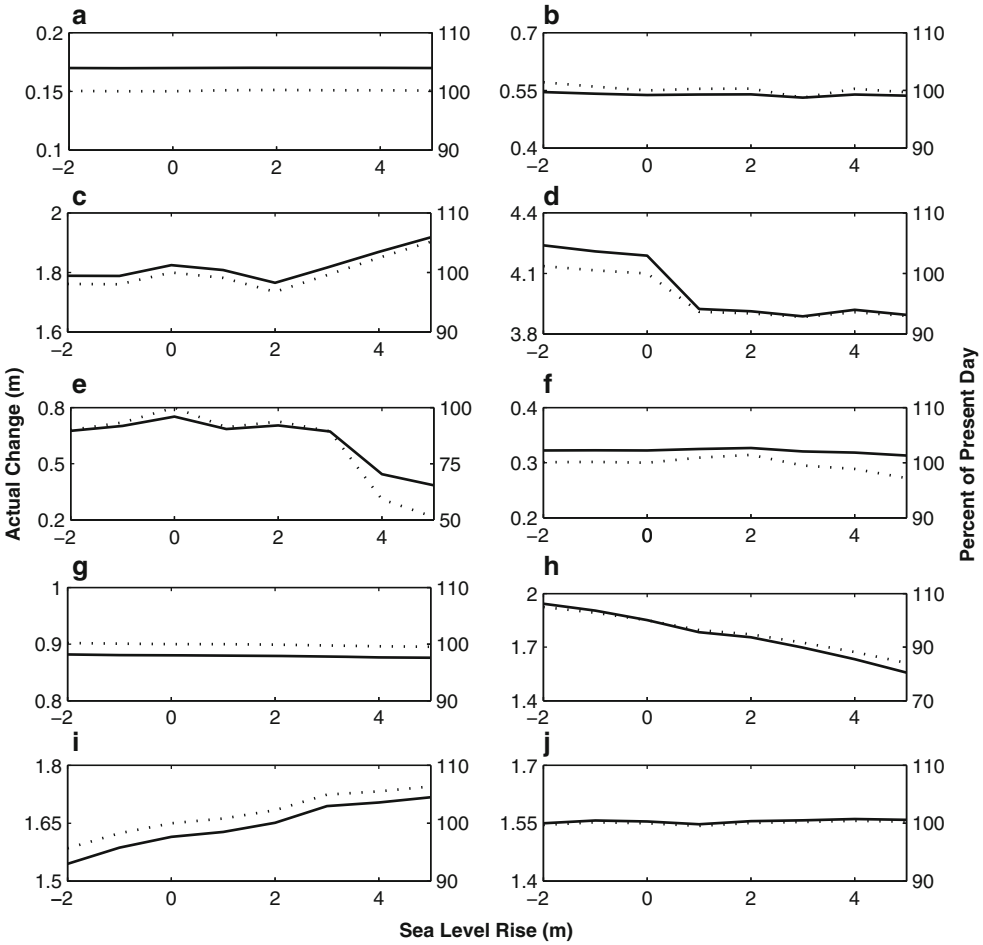

Fig. 4 M_2 SLR response curves for a number of locations on the shelf, plotted as actual change (*black line*) and percent of present day (*dotted line*), where **a** Atlantic Ocean, **b** North Sea, **c** Irish Sea, **d** Pentland Firth, **e** German Bight, **f** North Sea (mid), **g** Skagerrak, **h** Channel Isles, **i** English Channel and **j** Celtic Sea. Note the double *y*-axis, the right-hand axes correspond to the *dotted lines*

amphidromic point was set up to the northeast in the northern North Sea.

3.3 Results: energetics and stresses

At present day, the greatest velocities are found around headlands and into bays and along channels (Fig. 6). With 5-m SLR, the increases in astronomical tidal velocities observed in Morecambe Bay, in the Severn Estuary and in the Wash (all of which are estuaries in the UK) with 2-m SLR were not seen, most likely due to flooding of more land cells and hence a smaller tidal prism being funnelled up these channels/estuaries with 5-m SLR.

As expected, the spatial variation in bed shear stress mirrored that of tidal velocities; the greatest increases in the magnitudes of bed shear stresses were seen in estuaries in the 2-m SLR scenario, due to increased volumes of water being funnelled up the estuaries and channels. Significant decreases in bed shear stresses were seen in the area of the German Bight and along the northern coast of Holland and Germany, as well as in the English Channel, due to increased water depths. The increase in tidal velocities and hence bed shear stresses around headlands was far more pronounced with a SLR of 5 m.

The greatest increase in dissipation with 2-m SLR was again seen in estuaries (see Fig. 7). The greatest increase in maximum tidal energy dissipation occurred in the Bristol Channel/Severn Estuary (20% increase from the present-day maximum), in Morecambe Bay (70% increase from the present-day maximum), Solway Firth (88% increase from the present-day maximum) and in The Wash (100% increase from the present-day maximum).

A different spatial variation in tidal energy dissipation was found between the 2- and 5-m SLR scenarios (Fig. 7). There was significantly increased dissipation around headlands with 5-m SLR, associated with altered tidal currents. In contrast to the 2-m SLR scenario, with 5-m SLR, there was a general decrease in energy dissipation in the Bristol Channel/Severn Es-

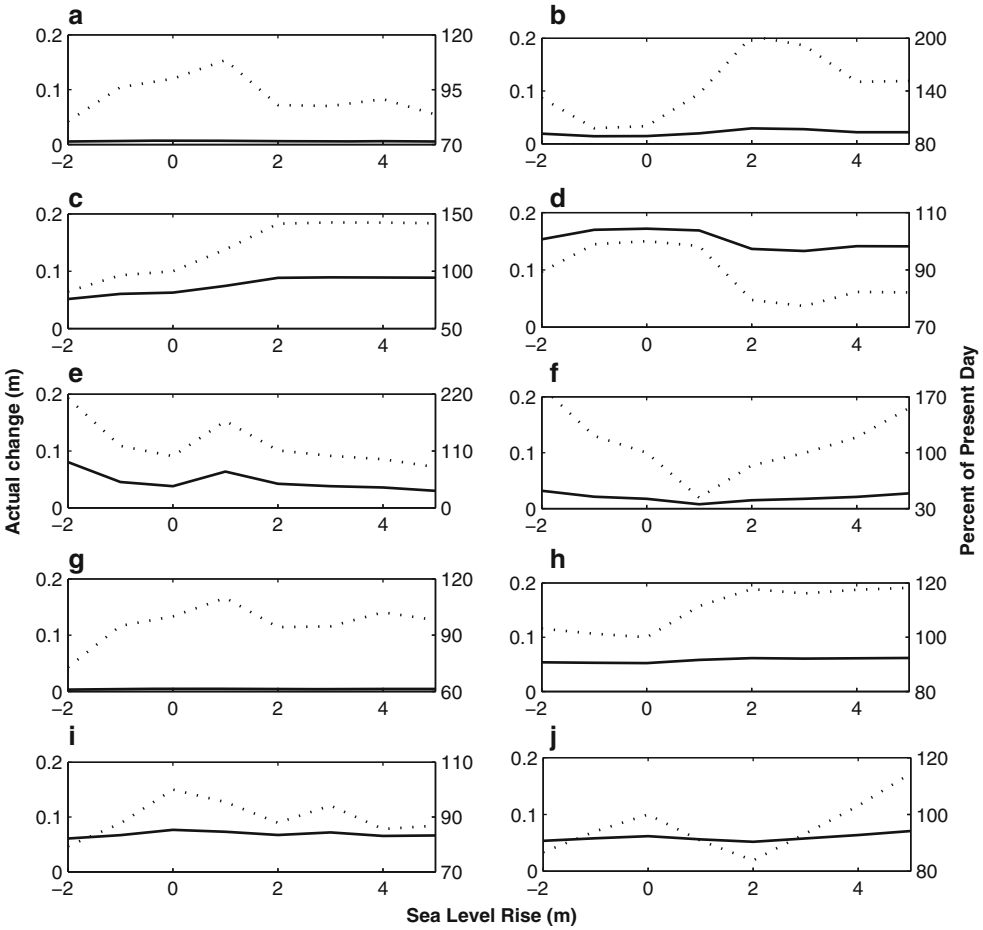

Fig. 5 M_4 SLR response curves for a number of locations on the shelf, plotted as actual change (*black line*) and percent of present day (*dotted line*), where **a** Atlantic Ocean, **b** North Sea, **c** Irish Sea, **d** Pentland Firth, **e** German Bight, **f** North Sea (mid), **g** Skagerrak, **h** Channel Isles, **i** English Channel and **j** Celtic Sea. Note the double *y*-axis; the right-hand axes correspond to the *dotted lines*

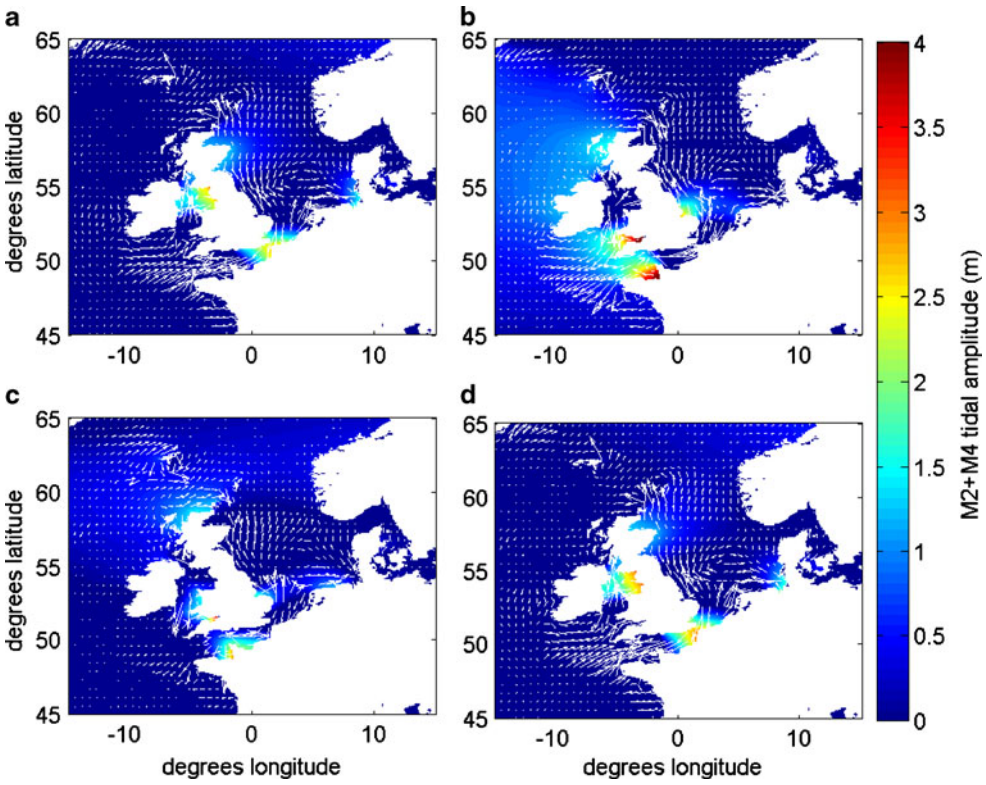

Fig. 6 Vector plot of astronomical tidal velocities overlying combined M_2 and M_4 amplitudes for present day where for **a** $T = 0$ h, **b** $T = 4$ h, **c** $T = 8$ h and **d** $T = 12$ h

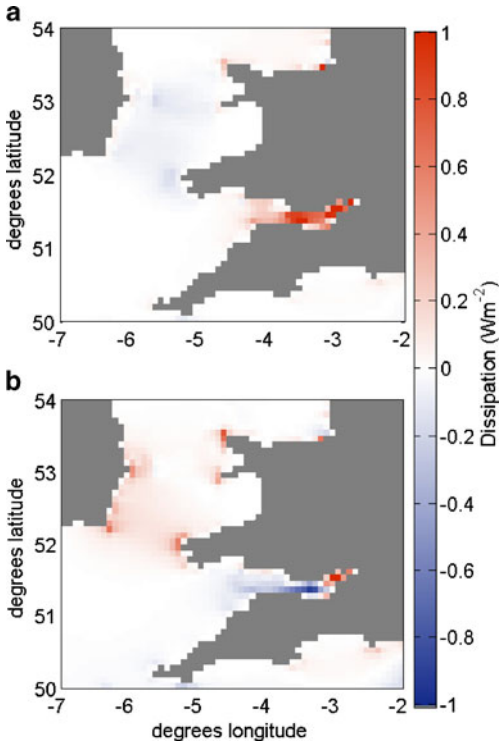

Fig. 7 Difference between average M_2 dissipation between 2-m SLR (**a**) and 5-m SLR (**b**) scenarios and present day in the St. George's Channel and the Bristol Channel

tuary (approximately 0.9 W m^{-2}) although an increase was seen at the head of the estuary (maximum increase of 1.14 W m^{-2} compared with the present-day values of approximately 4 and 0.8 W m^{-2} in the channel and at the head). There were also significant changes in dissipation in the area of the Orkney Islands (northeast of Scotland) with maximum increases and decreases of 1.91 and 3.77 W m^{-2} from present-day dissipation, respectively. There was significantly decreased dissipation in the English Channel in comparison to at present (approximately 0.5 W m^{-2}) as well as in the German Bight (1.13 W m^{-2}).

Note that these changes are all correlated to the changes in tidal amplitudes (Fig. 3) and thus related to either direct changes in tidal velocities or to flooding of new land cells (which in turn will impact on the tides). With SLR, the propagation speed of the tidal wave will increase—generally leading to enhanced dissipation rates—whereas flooding of new land cells will lead to significant dissipation in these cells. This will shift the amphidromic system towards the newly formed cells, thus enhancing the tides on the opposite side of the basin (see Taylor 1920 and Pelling et al. 2012, for detailed dynamical descriptions).

4 Impact of energy extraction and sea-level rise on the tides

4.1 Methods

The next step was to represent the extraction of energy from tidal power facilities in the Severn Estuary, Solway Firth and Morecambe Bay in the UK.

The Severn Estuary was used for the development of the method for implementing TPPs and for a number of sensitivity runs. For TPP implementation, the drag coefficient (c_d) was increased by the equivalent of 50 times for each of the model grids impounded upstream of the barrage over the area of energy extraction (in accordance with the methods of Sutherland et al. 2007 and Neill et al. 2009b). Such a large drag coefficient was chosen to represent a 'worst cast scenario' for the impacts of energy extraction on the tides. For the modelled 'Severn Barrage' (Fig. 8), c_d was thus set to 0.3 over the four grid cells of the barrage, whereas for the free-stream turbine simulations in the Morecambe Bay and Solway Firth, $c_d = 0.03$. A number of sensitivity tests were conducted for the Severn Barrage scheme, including varying the value of the drag coefficient and the shape of the barrage, implementing a wall to represent the physical structure of the barrage, as well as changing the water depth upstream and downstream of the barrage to represent local deposition and scouring, respectively. Of these sensitivity tests, the barrage shape found to have the most significant impact on the hydrodynamical regime was four grids that spanned the estuary in a straight line in the approximate location of the proposed Cardiff–Weston Barrage (Fig. 8d). To further increase how realistically the Severn Barrage was represented, the drag coefficient was only increased during the ebb tide to represent 'ebb generation' mode and the flow of water was blocked around the turning of high tide to represent the impounding of the water before generation commenced. Scouring and depositional effects were not represented within the final barrage runs although a wall was inserted. A value of 0.7 m s^{-1} was used to represent the 'cut-in speed' of the turbines, where tidal current velocities lower than the cut-in speed were not considered sufficient to drive the turbines (Douglas et al. 2008; Neill et al. 2009b).

We also considered free-stream TPPs in Solway Firth (SF) and in Morecambe Bay (MB) individually and together (denoted 'two bays'). We subsequently considered SF and MB in combination with energy extraction in the Severn Estuary (denoted 'three bays') for sensitivity tests and for comparison with the model results of Wolf et al. (2009). For the SF, MB and two bays runs, a drag coefficient of 0.3 was initially used, as

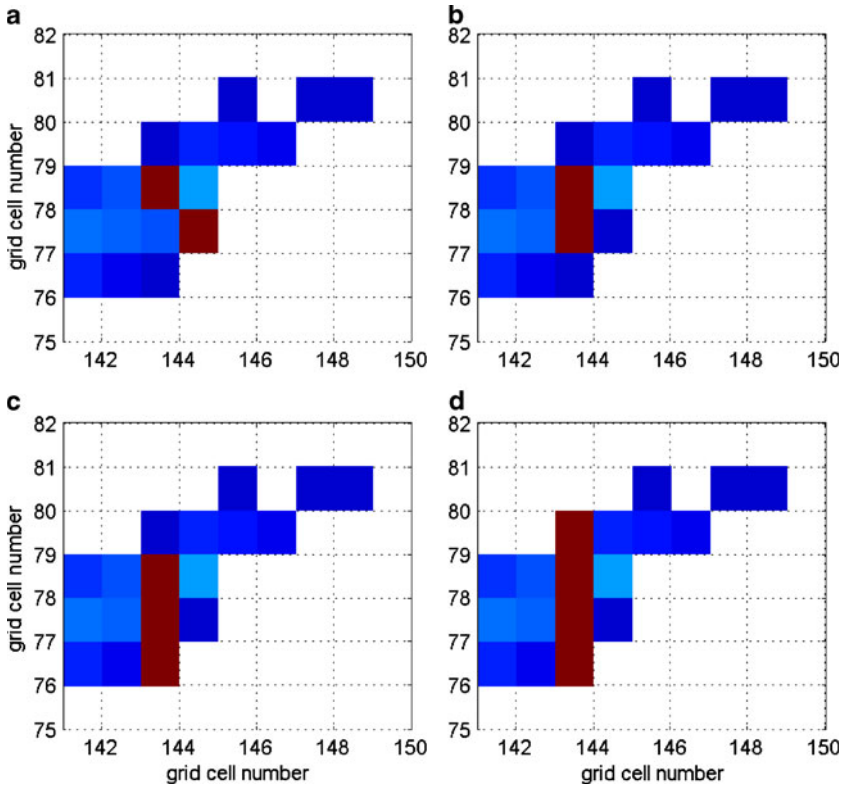

Fig. 8 **a–d** The model region of the Severn Estuary, showing the different shapes and locations used for TPP sensitivity testing. The *darker coloured cells* represent the location of the barrage. **d** The shape of the Severn Barrage used in the model runs for energy extraction in the Severn Estuary

per runs for the Severn Estuary. However, with such an extreme increase in drag coefficient, intended to represent the worst-case scenario of energy extraction for the Severn, the back effects on the tides with the three bays was unrealistically large—both spatially and in magnitude. Thus, for the three bays run, the drag coefficient was increased by only ten times the default, i.e. to 0.03, which better represented the less severe impact of energy extraction by tidal stream farms rather than tidal barrages. The drag coefficient was increased to this value on both the flood and the ebb tide (as we investigated free-stream TPPs).

Considering the model resolution, these methods were deemed sufficient for an initial investigation into the impacts of energy extraction in the Irish Sea on the tides of the northwest European shelf. The results of 2-m SLR in combination with the TPPs are compared with control runs for present day and 2-m SLR.

4.2 Results: Severn Barrage

With present-day sea levels and our assumed friction modifications, the tidal velocities upstream of the Severn Barrage reduced by around 20%, similar to the reduction of 24% modelled by Xia et al. (2010). Upstream of the barrage, the M_2 and S_2 amplitudes decreased by a maximum of 18% and 30%, respectively. Overall, there was decreased bed shear stress extending along the length of the Bristol Channel, associated with the reduced magnitude in the tidal currents. The tidal amplitude changes are similar to those with SLR only, with the exception of within the Bristol Channel (Fig. 3). Across the entire domain, the greatest decrease in M_2 tidal amplitude of 1.1 m was observed in the Severn Estuary, which equates to a 24% decrease. There was less of a discrepancy between the M_2 tidal amplitudes at 1- and 2-m SLR with the barrage in place in comparison to there being no barrage (Fig. 9), suggesting that the presence of the barrage has an effect on the reflection of the tidal wave within the estuary.

The red grid cells at the head of the estuary in Fig. 3b, c, e, f indicate the increase in tidal amplitude in newly flooded grid cells with SLR. The amplitude in these grid cells in the control run is negligible, and hence they are not shown in panels a and d.

As with the SLR only runs, there were increases in astronomical tidal velocities in many estuaries, with the exception of in the Severn Estuary where a decrease was observed as a result of the energy extraction. The greatest decrease in tidal velocities downstream of the Severn Barrage was a 17% decrease from present-day velocities. When considering SLR in parallel with the Severn Barrage, a significant increase in astronomical tidal velocities was observed between present day and

2-m SLR. This is in contrast with when the barrage was implemented without SLR, resulting in decreased tidal velocities, and is a consequence of the greater volume of water entering the region with increased sea levels. There was a significant decrease in bed shear stress in the area downstream of the barrage; an effect of the reduced tidal currents resulting from energy extraction at the barrage.

4.3 Results: Energy extraction in the Irish Sea

For MB only, at present-day sea level, there was minimal effect of energy extraction outside of the estuary (Figs. 10 and 11). The maximum decrease in M_2 tidal amplitude was 7% from present day in the locale of energy extraction. This effect is more pronounced with SLR, with a decrease of 15% within the impounded area in comparison to the 2-m SLR control run. The changes in tidal velocities, and hence dissipation, were also only local, with a maximum decrease of 11 W m^{-2} adjacent to (seawards of) the barrage. With no SLR, there was a significant increase in M_4 amplitude within MB (0.2 m) with energy extraction and a decrease in the M_4 amplitude up the northwest coast of the UK could be seen, the maximum of which was 0.06 m below the control run and was in the Firth of Clyde, western Scotland. With SLR there was the opposite impact on M_4 amplitude than with no SLR, with a decrease in MB and an increase in SF (0.09 m).

The maximum change in M_2 amplitude with SF in place is just seawards of the point of extraction, where a maximum of 0.12 m decrease in comparison to the control run was observed (Fig. 10). The effect on M_2 amplitude extended approximately 40 km west of the point of extraction. There were no significant changes in dissipation in any areas other than the model grid cells adjacent to the point of extraction. With 2-m SLR, the effect on the amplitude was spatially similar as for the control run but was more pronounced, with a decrease of 0.28 m within the area landwards of the TPP. There was also a resulting increase in tidal amplitude in the Irish Sea (along the eastern Irish coast), up to 0.06 m; the change in amplitude in this area was not significant in any other runs. The phase lines of M_4 moved more than the M_2 phase lines, with more of a difference with SLR. Dissipation patterns were similar for SLR as for the no SLR scenario. With 2-m SLR, there was a decrease in M_4 amplitude of up to 0.17 m within SF and a slight increase in M_4 amplitude in Liverpool Bay (0.05 m) was noted.

With MB and SF ('two bays'), the impact of energy extraction at both sites appeared to be approximately the combined effects of the individual runs. The same was found for the two bays 2-m SLR run except a significant far-field impact was observed (see Fig. 12). Along the east coast of Ireland, stretching right across the Irish Sea and into Cardigan Bay, there was a difference in M_2 amplitude of up to 0.09 m in comparison to the 2-m SLR run without TPPs. This

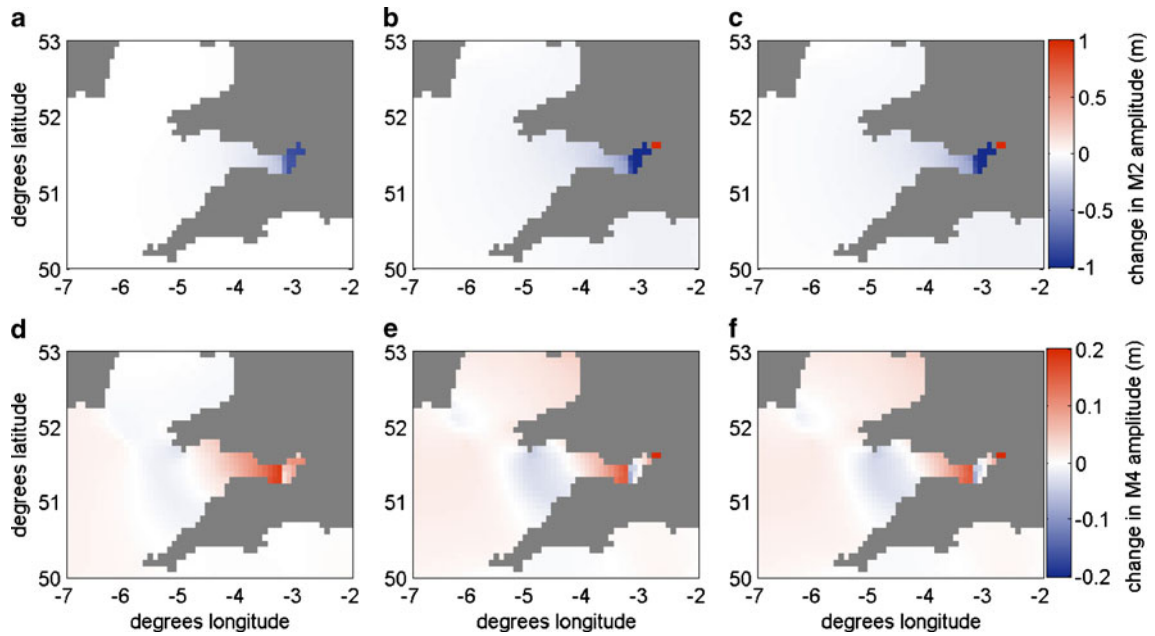

Fig. 9 Difference between M_2 (**a**–**c**) and M_4 (**d**–**f**) amplitudes with the Severn Barrage, present day (**a**, **d**), with 1-m SLR (**b**, **e**) and with 2-m SLR (**c**, **f**) and the control run. Note the different scales for the M_2 and M_4 panels

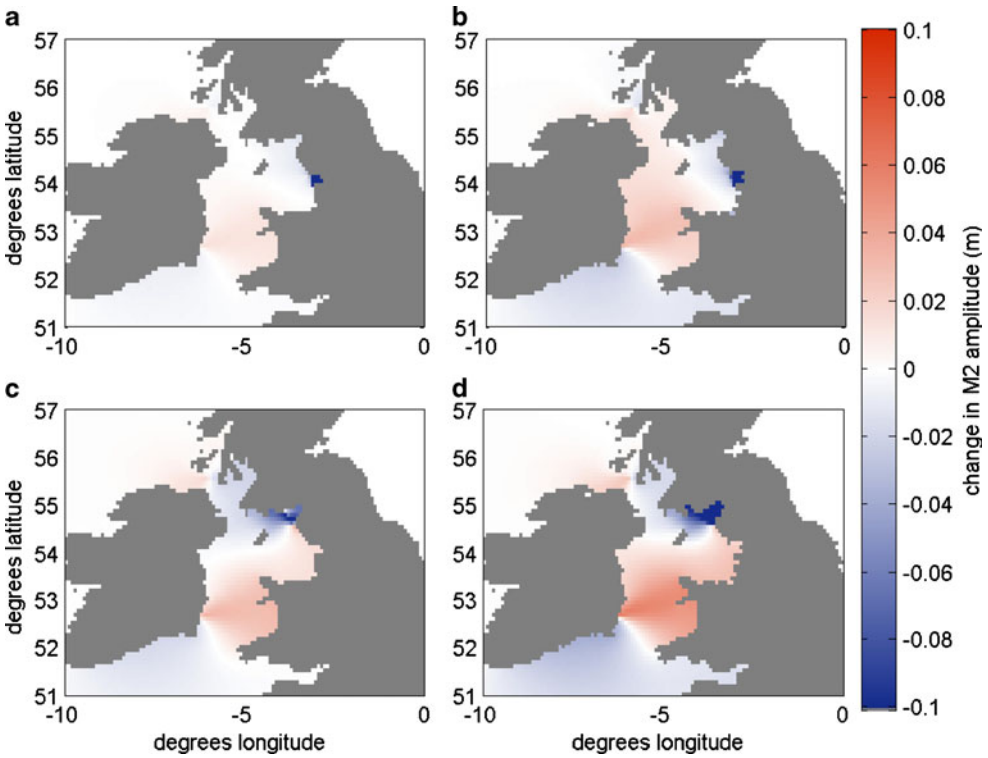

Fig. 10 Difference between M_2 amplitudes with Morecambe Bay (**a**, **b**) and Solway Firth (**c**, **d**) for present-day sea level (**a**, **c**) and 2-m SLR (**b**, **d**)

change in M_2 tidal amplitude is due to the westwards shift of the degenerate M_2 amphidromic point in the area, a result of extracting tidal energy in SF and MB (see the discussion at the end of Section 3.3). Also note that there were no far-field impact on velocities or tidal dissipation.

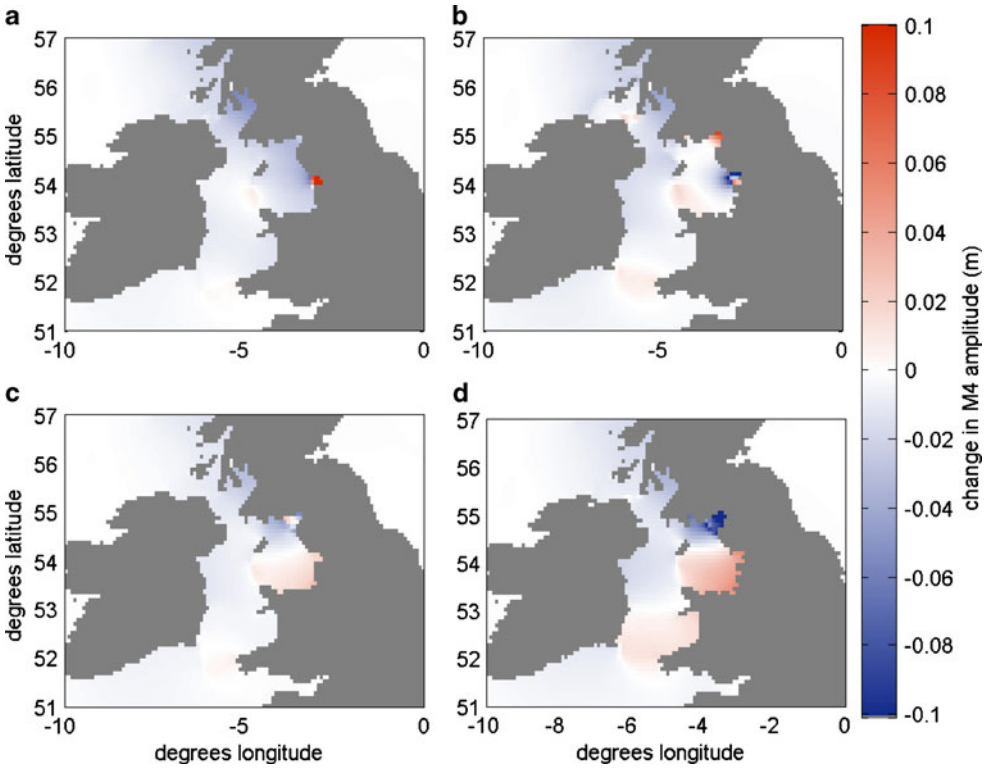

Fig. 11 Difference between M_4 amplitudes with Morecambe Bay (**a**, **b**) and Solway Firth (**c**, **d**) for present-day sea level (**a**, **c**) and 2-m SLR (**b**, **d**). Note the *different colour scales* to Fig. 10

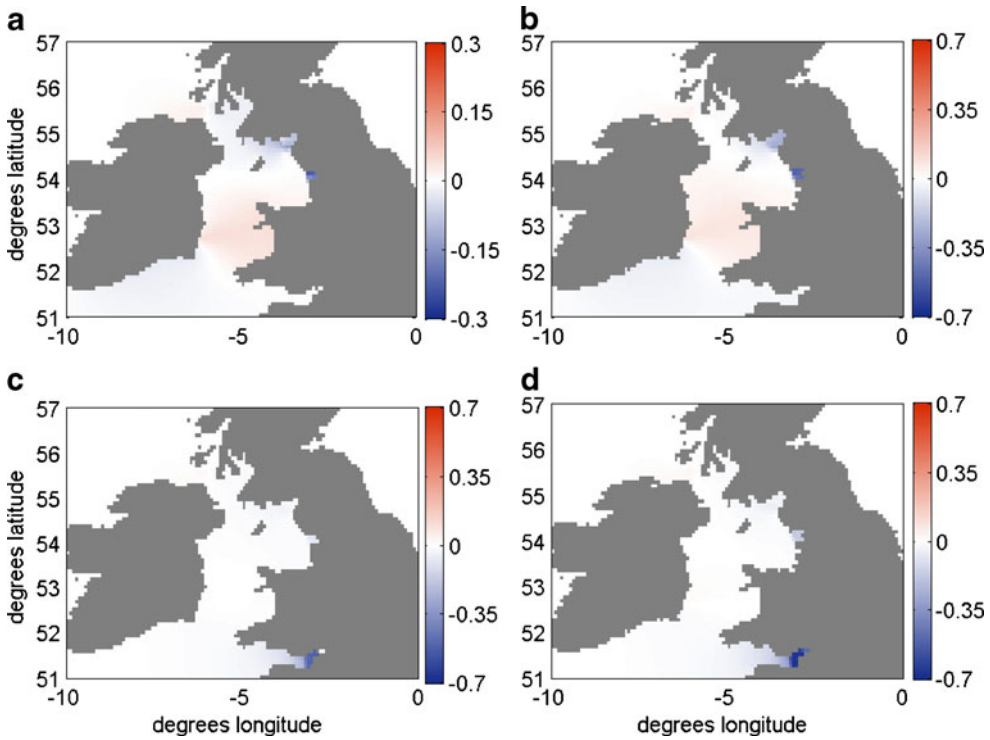

Fig. 12 Difference between M_2 amplitudes with two bays (**a**, **b**) and three bays (**c**, **d**) for present-day sea level (**a**, **c**) and 2-m SLR (**b**, **d**). Note that **a** has a different scale to **b**–**d**

With two bays, there was an increase in M_4 amplitude of 0.2 m with MB, and a slight decrease in and around SF although the effects extend further than with SF alone. There was also a decrease in M_4 amplitude of 0.09 m in the Firth of Clyde, north of the points of extraction. With 2-m SLR, there was a more significant increase in M_4 amplitude in Liverpool Bay (0.07 m), more significant decrease in SF and a different response within MB than the no SLR scenario. Further, there was a more pronounced decrease in M_4 amplitude along the western coast of Scotland than in the no SLR scenario.

With three bays, the most significant effect of energy extraction continues to be in the Severn Estuary (maximum amplitude change of 0.5 m decrease from the control run). Having energy extraction in three locations decreases the impact of energy extraction in SF and MB (individually or in the two bays run) as can be seen in Fig. 13. The impacts of two bays were thus reduced in three bays run due to the significant dissipation in the Severn Estuary due to energy extraction, resulting in reduced tidal energy propagating into the Irish Sea. There was significantly more change in the M_2 amplitude within MB in the three bays 2-m SLR scenario than present day, with a maximum of 0.17 m decrease (compared with insignificant changes in the present-day runs). The changes in M_2 amplitude in SF with 2-m SLR were only just around the accuracy of the model. With no SLR, the dissipation effects did not extend outside of the estuaries for MB and SF, but the decrease in dissipation in the Severn Estuary in comparison to present day (max decrease of 19 W m^{-2}) did extend towards the mouth of the estuary, similar to the spatial extent of the Severn Barrage alone run. With 2-m SLR, in the three bays scenario, there was increased dissipation in SF and MB in comparison to the no SLR scenario, although contrastingly, there was a decrease (15 W m^{-2}) in the dissipation in the Severn Estuary in comparison to the same run but with no SLR.

For present-day sea level, there were no significant changes in M_4 amplitude, except an increase in MB of 0.08 m (not shown). With 2-m SLR and three bays (again not shown), the only significant response in the M_4 amplitude was right in the head of the Severn Estuary, where a decrease of 0.12 m was found in comparison to the 2-m SLR control run.

As stated previously, when an area experiences an increased tidal dissipation, either due to bathymetric changes or due to artificially induced dissipation from a power plant, the amphidromic system will shift towards the area of enhanced dissipation. With SLR, there is significant flooding of new land around the bays investigated here. In combination with tidal power plants, we thus see a combined effect, which may be non-linear due to the feedback between dissipation and

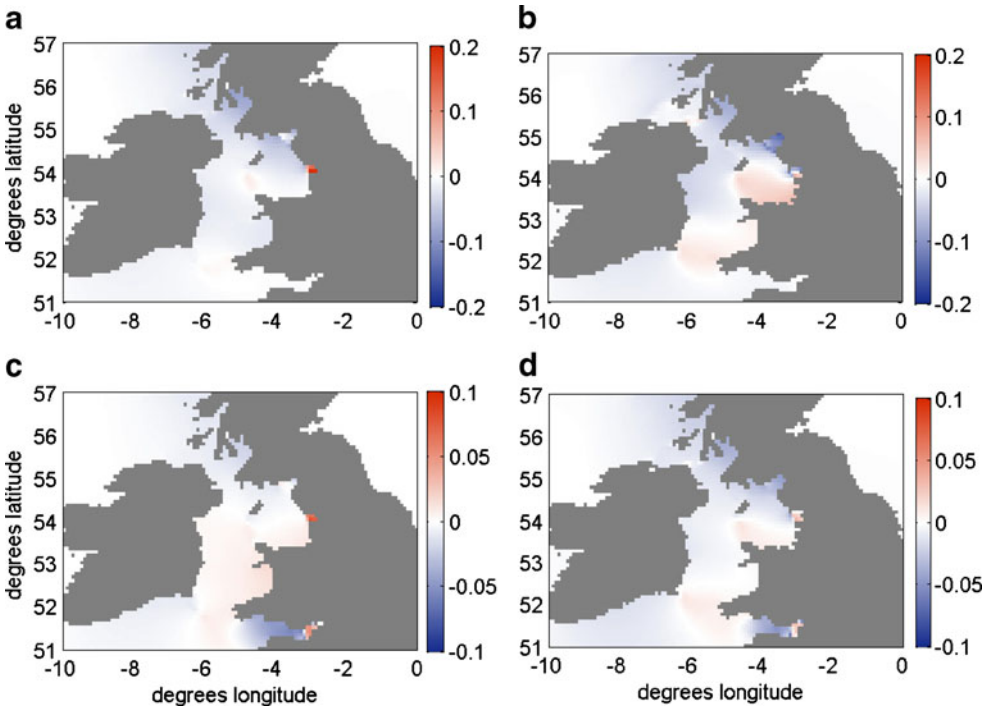

Fig. 13 Difference between M_4 amplitudes with two bays (**a**, **b**) and three bays (**b**, **d**) for present-day sea level (**a**, **c**) and 2-m SLR (**b**, **d**). Note the different scale to Fig. 12 and the different scales between the *upper* and *lower two panels*

tidal amplitudes. A more detailed investigation of these mechanisms are left for a future paper (Pelling et al. 2012).

5 Discussion

A numerical tidal model is used to investigate the impact on the tides of SLR and tidal power extraction on the European shelf. Migration of amphidromic points occurs since their locations are dependent upon the interaction between the incident and reflected tidal waves and hence are influenced by water depth, frictional effects and topography (Hendershott and Speranza 1971; Pelling and Green 2012). Thus, as sea levels change or as frictional effects are varied, such as through the implementation of tidal power plants, tidal phase lines and the location of amphidromic points can be affected. The changes in tidal amplitudes are attributed to a shift in the amphidromic points, as well as to resonant effects, in keeping with the model results of Roos and Schuttelaars (2011) for semi-enclosed basins. Changes to the damping are in accordance with the observed increase in tidal velocities in channels and estuaries with increasing sea levels, where the increased volume of water is funneled along the channel. It is likely that the response of the M_2 (and to a lesser extent, S_2) tidal amplitudes along the eastern coast of the UK with increasing sea levels is influenced by the eastwards shift of the M_2 amphidromic point in the North Sea. Significantly increased tidal velocities in such areas will cause an increased bed shear stress and dissipation, the latter of which increases the damping effect on the tide, hence decreasing the amplitudes. Changes to the bed shear stress would likely have implications for large-scale sediment transport on the shelf, an impact which has been left for future studies.

A linear relationship has been observed between the area of tidally mixed waters and SLR. There is a decrease in the surface area of mixed waters on the European shelf as sea levels rise; for instance, between the present day and 2-m SLR, the area of mixed waters decreased by approximately 1%, which could have significant implications for shelf sea biogeochemistry.

A number of the results obtained in this study are in contrast with the findings of Pickering et al. (2012) who used Delft3D and unpublished results using OTIS (Egbert et al. 2004; Green 2010). For example, both these models show changes in the German Bight and in the Irish Sea with the opposite sign to the results in this paper. Both these previous investigations differ from the present in that we allow land to flood with rising sea levels, thus forming new wet cells; the previous studies (Green 2010; Pickering et al. 2012) added vertical walls at the present coastline and then raised the sea level. When KUTM was run with this no flooding of land cells, the results of Pickering et al. (2012) were recreated. These differences in the implementation of

SLR appear to have a significant effect on the response of the tides. Further analysis of the response on the European shelf is left for a comparison paper (Pelling et al. 2012), but Pelling and Green (2012) have reported similar effects in the Bay of Fundy.

The impact upon the tides of increasing sea levels also has implications for tidal power extraction through changes to tidal amplitudes and velocities although only the combined impacts of energy extraction in SF and MB seemed to have any significant non-local effect on the tides. These results highlight the importance of considering other tidal power plants when looking into the impacts of energy extraction on the tidal regime in a particular estuary as the effects may be a non-linear combination of more than one tidal power plant.

Although the RMS error of the model is low, increased accuracy would improve the comprehensiveness of the results and the quantitative estimates of impacts. In addition, a higher resolution model would facilitate more accurate representation of the coastline. Changing the sea level within the model varied the water level uniformly across the entire domain which is not entirely realistic as SLR varies spatially since other factors such as isostatic rebound also occur.

The findings presented here suggest that SLR may significantly alter the pattern of the shelf tides, although the effects do not appear to extend to the open ocean. It has also been suggested that the way SLR is implemented within tidal models may provide significantly different results, but we do not argue for either method being the correct one: that is a political question. Changes in sea level can affect the tidal regimes, energy dissipation, the biogeochemical system, sediment transport, as well as the tidal power potential of the northwest European shelf seas. The results are significant when conducting feasibility studies and impact studies of various tidal power schemes.

Acknowledgements Funding was provided by the Natural Environment Research Council (NERC) through grants NE/I527853/1 (Ph.D. studentship to SLW), NE/H/524549/1 (Ph.D. studentship to HEP) and NE/F/014821 (advanced fellowship to JAMG). SLW also acknowledges a NERC M.Sc. studentship, and JAMG receives support from the Climate Change Consortium for Wales. Katsuto Uehara provided invaluable modelling support.

References

Andersen OB (1999) Shallow water tides in the northwest European shelf region from Topex/Poseidon altimetry. J Geophys Res 104(4):7729–7741. doi:10.1029/1998JC900,112

Arbic BK, Garrett C (2009) A coupled oscillator model of shelf and ocean tides. Cont Shelf Res 30(6):564–574

Bindoff N, Willebrand J, Artale V, A C, Gregory J, Gulev S, Hanawa K, Qu CL, Levitus S, Nojiri Y, Shum C, Talley L, Unnikrishnan A (2007) Observations: oceanic climate change and sea level. In: Solomon S, Qin D, Manning M, Chen Z, Marquis M, Averyt KB, Tignor M, Miller HL (eds) The physical science basis. Contribution of working group I to the fourth assessment report of the intergovernmental panel on climate change. Cambridge University Press, Cambridge

Burrows R, Walkington I, Yates N, Hedges T, Chen D, Li M, Zhou J, Wolf J, Proctor R, Holt J, Prandle D (2009) Tidal energy potential in UK waters. Proc. Inst Civ Eng Marit Eng 162(MA4):155–164. doi:10.1680/maen.2009.162.4.155

Church JA, White NJ (2006) A 20th century acceleration in global sea-level rise. Geophys Res Lett 33:L01, 602

Douglas CA, Harrison GP, Chick JP (2008) Life cycle assessment of the Seagen marine current turbine. Proc Inst Mech Eng Proc A J Eng Marit Env 222:1–12. doi:10.1243/14750,902JEME94

Egbert GD, Erofeeva SY (2002) Efficient inverse modeling of barotropic ocean tides. J Atmos Ocean Tech 19(2):183–204

Egbert GD, Ray RD (2001) Estimates of M2 tidal energy dissipation from TOPEX/Poseidon altimeter data. J Geophys Res 106:22,475–22,502

Egbert GD, Bills BG, Ray RD (2004) Numerical modeling of the global semidiurnal tide in the present day and in the last glacial maximum. J Geophys Res 109:C03,003. doi:10.1029/2003JC001,973

Gehrels R (2010) Sea-level changes since the last glacial maximum: an appraisal of the IPCC fourth assessment report. J Quat Sci 25(1):26–38. doi:10.1002/jqs.1273

Gehrels WR, Milne GA, Kirby JR, Patterson RT, Belknap DF (2004) Late Holocene sea-level changes and isostatic crustal movements in Atlantic Canada. Quat Int 120:79–89. doi:10.1016/j.quaint.2004.01.008

Green JAM (2010) Ocean tides and resonance. Ocean Dyn 60(5):1243-1253 doi:10.1007/s10,236-010-0331-1

Green JAM, Green CL, Bigg GR, Rippeth TP, Scourse JD, Uehara K (2009) Tidal mixing and the meridional overturning circulation from the last glacial maximum. Geophys Res Lett 36:L15,603. doi:10.1029/2009GL039,309

Griffiths S, Peltier W (2008) Megatides in the Arctic Ocean under glacial conditions. Geophys Res Lett 35 (L08605)

Griffiths S, Peltier W (2009) Modeling of polar ocean tides at the last glacial maximum: amplification, sensitivity, and climatological implications. J Climate 22(11):2905–2924

Hall P, Davies AM (2004) Modelling tidally induced sediment-transport paths over the northwest European shelf: the influence of sea-level reduction. Ocean Dyn 54:126–141. doi:10.1007/s10,236-003-007-7

Hasegawa D, Sheng J, Greenberg DA, Thompson KR (2011) Far-field effects of tidal energy extraction in the Minas Passage on tidal circulation in the Bay of Fundy and Gulf of Maine using a nested-grid coastal circulation model. Ocean Dyn 61:1845–1868. doi:10.1007/s10,236-011-0481-9

Hendershott MC, Speranza A (1971) Co-oscillating tides in long, narrow bays; the Taylor problem revisited. Deep-Sea Res 18:959–980

Hunter J (2009) Estimating sea-level extremes under conditions of uncertain sea-level rise. Clim Change 99(3):331–350. doi:10.1007/s10,584-009-9671-6

Van Landeghem KJJ, Uehara K, Wheeler AJ, Mitchell NC, Scourse JD (2009) Post-glacial sediment dynamics in the

Irish Sea and sediment wave morphology: data-model comparisons. Cont Shelf Res 29(14):1723–1736. doi:10.1016/j.csr.2009.05.014

Lane A, Prandle D (2007) Changing flood risks in estuaries due to global climate change: forecasts from observations, theory and models. Int J Appl Math Eng Sci 1(11):69–88

Miller L, Douglas BC (2004) Mass and volume contributions to twentieth-century global sea level rise. Nature 428:406–409

Milne G, Gehrels WR, Highes CW, Tamisiea ME (2009) Identifying the cause of sea-level change. Nat Geosci 2:471–476. doi:10.1038/ngeo544

Mitchell AJ, Ulic D, Hampson GJ, Allison PA, Groman GJ, Piggott MD, Wells MR, Pain CC (2010) Modelling tidal current-induced bed shear stress and palaeocirculation in an epicontinental seaway: the Bohemian Cretaceous basin, central Europe. Sedimentology 57:359–388. doi:10.1111/j.1365-3091.2009.01,082.x

Muller M, Haak H, Jungclaus JH, Sundermann J, Thomas M (2010) The effect of ocean tides on a climate model simulation. Ocean Model 35:304–313 doi:10.1016/j.ocemod.2010.09.001

Neill SP, Scourse JD, Bigg GR, Uehara K (2009a) Changes in wave climate over the northwest European shelf seas during the last 12,000 years. J Geophys Res 114:19. doi:10.1029/2009JC005,288

Neill SP, Litt EJ, Couch SJ, Davies AG (2009b) The impact of tidal stream turbines on large-scale sediment dynamics. Renew Energy 34:2803–2812. doi:10.1016/j.renene.2009.06.015

Nerem RS, Leuliette E, Cazenave A (2006) Present-day sea-level change: a review. Compt Rendus Geosci 338:1077–1083. doi:10.1016/j.crte.2006.09.001

Pelling HE, Green JAM (2012) Sea level rise, tidal power, and resonance in the gulf of maine. J Geophys Res (in revision)

Pelling HE, Green JAM, Ward SL (2012) A mechanistic description of the impact of sea level rise on shelf sea tides. Ocean Model (in revision)

Pfeffer WT, Harper JT, O'Neel S (2008) Kinematic constraints on glacier contributions to 21st-century sea-level rise. Science 321:1340–1342. doi:10.1126/science.1159,099

Pickering M, Wells N, Horsburgh K, Green J (2012) The impact of future sea-level rise on the European shelf tides. Cont Shelf Res 35:1–15. doi:10.1016/j.csr.2011.11.011

Pingree RD, Griffiths DK (1979) Sand transport paths around the British Isles resulting from M2 and M4 tidal interactions. J Mar Biol 59:497–513

Pingree RD, Griffiths DK (1982) Tidal friction and the diurnal tides on the north-west European shelf. J Mar Biol 62:577–593

Prandle D (2009) Design of tidal barrage power schemes. Proc Inst Civil Eng Mar Eng 162:147–153. doi:10.1680/maen.2009.162.4.147

Pugh DT (1996) Tides, surges and mean sea level. Wiley, New York

Rippeth TP, Scourse JD, Uehara K, McKeown S (2008) Impact of sea-level rise over the last deglacial transition on the strength of the continental shelf CO_2 pump. Geophys Res Lett 34(24):4. doi:10.1029/2008GL035,880

Roos PC, Schuttelaars HM (2011) Influence of topography on tide propagation and amplification in semi-enclosed basins. Ocean Dyn 61:21–38. doi:10.1029/2008GL035,880

Ross V (2011) Tuning tidal turbines in-concert to maximise farm efficiency. J Fluid Mech 671:587–604. doi:10.1017/S0022112010006,191

Stern N (2007) Stern review on the economics of climate change, HM treasury. Cambridge University Press, Cambridge

Sutherland G, Foreman M, Garrett C (2007) Tidal current energy assessment for Johnstone Strait, Vancouver Island. Power Energ 221:147–157

Taylor, GI (1920). Tidal oscillations in gulfs and rectangular basins. Proc Lond Math Soc 20:148–181

Uehara K, Scourse JD, Horsburgh KJ, Lambeck K, Purcell AP (2006) Tidal evolution of the northwest European shelf seas from the last glacial maximum to the present. J Geophys Res 111:C09,025. doi:10.1029/2006JC003,531

van der Molen J (2002) The influence of tides, wind and waves on the net sand transport in the North Sea. Cont Shelf Res 22:2739–2762

Vermeer M, Rahmstorf S (2009) Global sea level linked to global temperature. Proc Natl Acad Sci 106(51):21527–21532. doi:10.1073/pnas.0907765106

Wolf J, Walkington IA, Holt J, Burrows R (2009) Environmental impact of tidal power schemes. Proc Inst Civil Eng Mar Eng 162:165–177

Xia J, Falconer RA, Lin B (2010) Impact of different tidal renewable energy projects on the hydrodynamic processes in the Severn Estuary, UK. Ocean Model 32:86–104. doi:10.1016/j.ocemod.2009.11.002